Presentación de proyectos para la clase de Modelado y Simulación

Generación 2014

DCA - Cinvestav
rcadena@ctrl.cinvestav.mx

Capítulo 1

Benford's Law in Dynamical Systems

Emanuel Rocha Campos, Gerardo E. Cardona Sánchez

I. Overview

The purpose of this document is to present the results of simulations and experiments regarding the implementation of a physical dynamical system, in this case, an autonomous electronic circuit made in order to look for Benford's Law conformity of a physical quantity. The circuits that were chosen for this objective have various regions of operation and can be easily regulated, so an important amount of experiments and simulations were performed. Conformity to Benford's Law was achieved, and the circumstances under which the satisfactory results were obtained are also described in this document.

I. Benford's Law

Benford's Law, also called the First Digit Law refers to the frequency distribution of digits from a data source. The first observation was made by Benford [1] who looked through various sources of data and found that in some data sets the number 1 repeated about 30 % of the time, while larger digits occur less frequently.

Benford's Law is the probability distribution for the mantissa with respect to base $b \in \mathbb{N}\ \ 1$ given by $\mathbb{P}(\text{mantissa}_b \leq t) = \log_b t \forall t \in [1, b]$; the special case dealt with in this document is that described by:

$$\mathbb{P}(\text{first significant digit}_{10} = d) = \log_{10}(1 + \frac{1}{d}), d = 1, ..., 9$$

Today, this distribution is used in accounting fraud detection[2], Election data and Genome data. Also, a relation between the brain electrical activity and Benford's Law was encountered, and the researches noted that compliance with Benford's Law is influenced by the presence of the anesthesic sevoflurane, or destroyed by noise in the EEG[3].

We give two examples where Benford's Law holds: the well known Fibonacci sequence, and population data from Mexico's Municipalities, obtained from INEGI.

Fibonacci Sequence

The Fibonacci sequence consists in the sequence: 1,1,2,3,5,8,13,21,34,55,89,144, ... ; where the sequence can be defined as the recurrence relation:

$$f_n = f_{n-1} + f_{n-2}$$

Next, the most significant digit from the first 1000 Fibonacci numbers is obtained, and the frequency of repetition of number 1 as the first digit is calculated, the same can be done with number 2, and so on until number 9. Finally a plot of this frequency distribution against the distribution predicted by Benford's Law is presented.

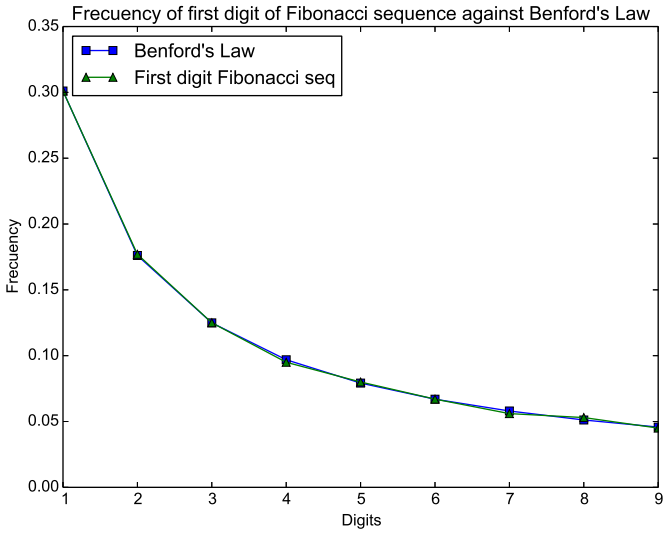

Figura 1.1: *Fibonacci Sequence against Benford's Law*

Mexico's Municipalities Population

From the Mexico's National Institute of Geography and Statistics, INEGI, data from the 2010 census can be obtained. That year, 2351 Municipalities where censused and information is freely available at the institute web page.

As with the first example, the most significant digit of the population of each municipality was taken, and the frequency of repetition of each digit between 1 and 9 was compared with the prediction made by Benford's Law.

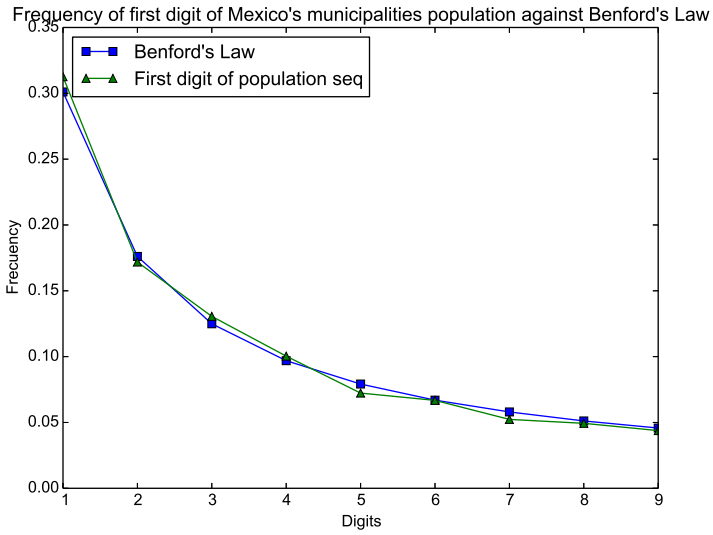

Figura 1.2: *Fibonacci Sequence against Benford's Law*

II. Autonomous Circuits

An Autonomous Circuit is a circuit that produces a time-varying output without having a time-varying input[6]. More formally:

An electronic circuit is described by a system of ordinary differential equations of the form:

$$\dot{\mathbf{X}}(t) = \mathbf{F}(\mathbf{X}(t), t)$$

Where $\mathbf{X}(t) = (X_1(t), X_2(t), ..., X_n(t))^T \in \mathbb{R}$ is called the *state vector* and $\mathbf{F}$ is called the *vector field*. $\dot{\mathbf{X}(t)}$ denotes the derivative of $\mathbf{X}(t)$ with respect to time.

If the vector field $\mathbf{F}$ depends explicitly on t, then the system is said to be *non-autonomous*. If the vector field depends only on the state and is *independent* of time t, then the system is said to be *autonomous* and may be written in the simpler form:

$$\dot{\mathbf{X}} = \mathbf{F}(\mathbf{X}) \tag{1.1}$$

The time evolution of the state of an autonomous electronic circuit from an initial point $\dot{\mathbf{X}}$ at t=0 is given by

$$\phi(\mathbf{X_0}) = \mathbf{X_0} + \int_o^t \mathbf{F}(\mathbf{X}(\tau))d\tau, t \in \mathbb{R}_+$$

The solution $\phi(\mathbf{X_0})$ is called a *trajectory* through $\mathbf{X_0}$, and the set $\phi(\mathbf{X_0}), t \in \mathbb{R}_+$ is an *orbit* of the system (1.1). The collection of maps ϕ_t that describe the evolution of the entire state space with time is called the *flow*.

An autonomous electronic circuit is an example of a *deterministic dynamical system*.

III. Defining Chaos

Chaos is aperiodic long-term behavior in a determinisic system that exhibits sensitive dependence on initial conditions [4]

- *Aperiodic long-term behavior* means that there are trajectories which do not settle down to fixed points, periodic orbits, or quasiperiodic orbits as *t*->ínf.
- *Deterministic* means that the system has no random or noisy inputs or parameters. The irregular behavior arises from the system's nonlinearity, rather than from noisi driving forces.
- *Sensitive dependence on initial conditions* means that nearby trajectories separate exponentially fast, i.e., that the system has a positive Lyapunov Exponent

Lyapunov Exponent

The lyapunov exponent of a dynamical system is a quantity that characterizes the rate of separation of infinitesimally close trayectories[5].

Suppose that we let transients decay, so that a trajectory is *on* the attractor. Suppose $\mathbf{Œ}(x,t)$ is a point on the attractor at time t, and consider a nearby point $\mathbf{Œ}(t)+\delta(t)$ where δ is a very small separation. It can be seen in the following figure, that $\delta(t)$ grows. The two trajectories diverge with at a rate given by

$\|\delta(t)\| \ \|\delta_o o\| e^{\lambda t}$

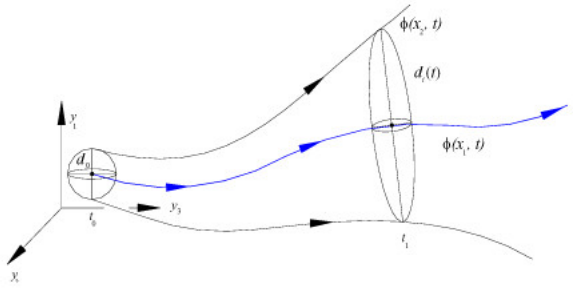

Figura 1.3: *Neighboring trajetories separating exponentially fast with initial separation* δ_0

When at least one Lyapunov exponent is positive the attractor possesses the property of sensitive dependence of initial conditions.

Chua's Circuit

- **Chua's Oscillator**
  Leon Chua did research regarding Lorenz's equations[7][6], and deviced a chaotic electronic circuit with only one non-linear element, which is a 5-segment piecewise-linear resistor.

  The dynamics of the system can be modeled by the system of three nonlinear ordinary differential equations:

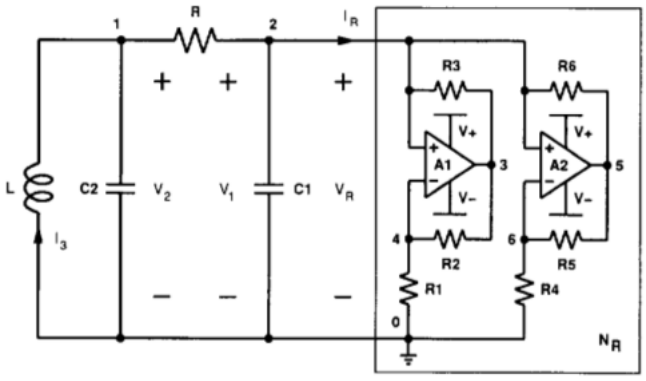

Figura 1.4: *Schematic of Chua's Circuit*

$$\frac{dV_1}{dt} = \frac{G}{C_1}(V_2 - V_1) - \frac{1}{C_1}f(V_1) \tag{1.2}$$

$$\frac{dV_2}{dt} = \frac{1}{C_2}I_3 - \frac{G}{C_2}(V_2 - V_1) \tag{1.3}$$

$$\frac{dI_3}{dt} = -\frac{1}{L}V_2 \tag{1.4}$$

$$\tag{1.5}$$

with $G = \frac{1}{R}$ and $f(V_1)$ is given by:

$$\begin{aligned} \frac{G}{C1}V_2 - \frac{G'_b}{C_1}V_1 - (\frac{G_b - G_a}{C_1})E \quad & if \quad V_1 < -E \\ \frac{G}{C1}V_2 - \frac{G'_a}{C_1}V_1 \quad & if \quad -E \geq v1 \leq E \\ \frac{G}{C1}V_2 - \frac{G'_b}{C_1}V_1 - (\frac{G_a - G_b}{C_1})E \quad & if \quad V_1 > E \end{aligned}$$

- **Properties**

1. **Nonlinearity:** The system of equations has a nonlinear 2-terminal resistor described by a three segment piecewise-linear v-i characteristic shown in the following figure:
   The piecewise-linear nature of the nonlinearity in Chua's Oscillator divides the state-space of the circuit into three distinct affine regions ($V_1 < E$), ($\|V_1\| < E$) and ($V_1 > E$)
2. **Symmetry:**The piecewise-linear function is symmetric with respect to the origin, there exists three equilibrium points, at 0, P_- and P_+. In the following figure, a double scroll Chua's attractor is shown. Since three equilibrium points are involved, this attractor is symmetric with respect to the origin

3. **Dissipativity**

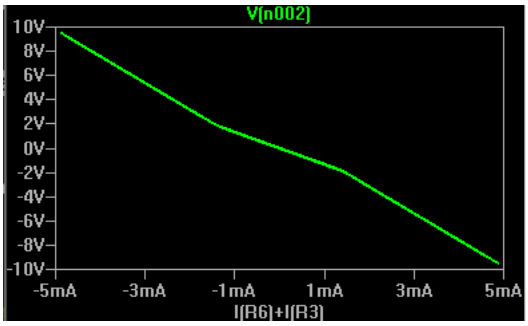

Figura 1.5: *v-i characteristic of the non-linear resistor*

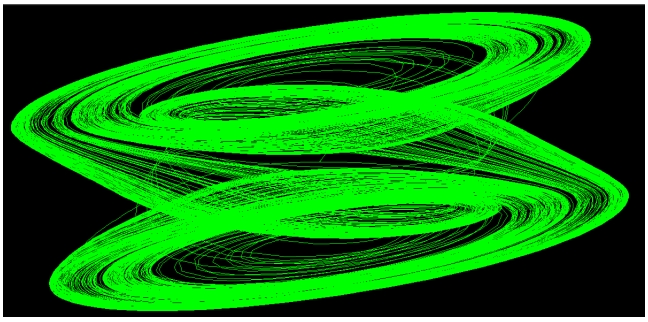

Figura 1.6: *v-i characteristic of the non-linear resistor*

Takougang Circuit

- **Three-dimensional autonomous system by Takougang et. al.** A three-dimensional autonomous system is presented by Sifei Takougang Kingni[8]. The system exhibits chaotic bursting oscillations.
  The three-dimensional system is described as follows:

$$\frac{dx}{dt} = -x + y \tag{1.6}$$

$$\frac{dy}{dt} = xz - cy \tag{1.7}$$

$$\frac{dz}{dt} = b - x^2 - dz \tag{1.8}$$

  where $b, c, d \in \mathbb{R}$

- **Properties**
  - **non-linearity:** Non-linearity given by the term x^2 and xz
  - **symmetry:** Under the transformation defined by $(x, y, z) \to (-x, -y, -z)$, the system has a natural symmetry
    Next, we show that the system is symmetric.
    Definition: Let f be a smooth function $f : \mathbb{R}^n \to \mathbb{R}^n$ and let

$$\dot{\mathbf{x}} = f(\mathbf{x})$$

be a system of ordinary differential equations. In addition, let γ be an invertible matrix. Then γ is a *symmetry* of the ordinary differential equation if

$$f(\gamma \mathbf{x}) = \gamma f(\mathbf{x})$$

Now, given the equation of the three-dimensional autonomous system, under the transformation $(x, y, z) \to (-x, -y, -z)$, to verify that this transformation is a symmetry of the autonomous equation, we observe that the symmetry is associated with the matrix γ defined as

$$\gamma = \begin{bmatrix} -1 & 0 & 0 \\ 0 & -1 & 0 \\ 0 & 0 & 1 \end{bmatrix} \tag{1.9}$$

let

$$\dot{\mathbf{x}} = f(\mathbf{x}) = \begin{bmatrix} -x + y \\ xz - cy \\ b - x^2 - dz \end{bmatrix} \tag{1.10}$$

with $\mathbf{x}^T = (x, y, z)$
Now, we proceed to show that $\gamma f(\mathbf{x}) = f(\gamma \mathbf{x})$:
On the left hand side:

$$\begin{aligned} \gamma f(\mathbf{x}) &= \begin{bmatrix} -1 & 0 & 0 \\ 0 & -1 & 0 \\ 0 & 0 & 1 \end{bmatrix} \begin{bmatrix} -x + y \\ xz - cy \\ b - x^2 - dz \end{bmatrix} \\ &= \begin{bmatrix} x - y \\ -xz + cy \\ b - x^2 - dz \end{bmatrix} \end{aligned}$$

And now, on the right hand side:

$$\begin{aligned} f(\gamma \mathbf{x}) &= f\left(\begin{bmatrix} -1 & 0 & 0 \\ 0 & -1 & 0 \\ 0 & 0 & 1 \end{bmatrix} \begin{bmatrix} x \\ y \\ z \end{bmatrix} \right) \\ &= f\left(\begin{bmatrix} x \\ y \\ z \end{bmatrix} \right) \qquad\qquad = \begin{bmatrix} x - y \\ -xz + cy \\ b - x^2 - dz \end{bmatrix} \end{aligned}$$

Since the left hand side is equal to the right hand side, then γ is a symmetry of the Three-dimensional Autonomous System. In other words, all solutions are either symmetric themselves, or have a symmetric partner

- **Dissipativity** The system with the general condition for dissipativity (or Volume contraction):

$$\begin{aligned}\nabla V &= \frac{\partial(\frac{dx}{dt})}{\partial x} + \frac{\partial(\frac{dy}{dt})}{\partial y} + \frac{\partial(\frac{dz}{dt})}{\partial z} \\ &= -(1+c+d)\end{aligned}$$

So

$$\begin{aligned}V'(t) &= -(1+c+d)V \\ V(t)V(0)e^{-(1+c+d)}t\end{aligned}$$

Thus volumes in phase space shrink exponentially fast An explanation of dissipativity is given in [4] page 320.

- **Fixed Points** The system has two types of fixed points:

$$\begin{aligned}0 &= -x + y && \Rightarrow x = y \\ 0 &= xz - cy && \Rightarrow z = c \\ 0 &= b - x^2 - dz && \Rightarrow x^2 + dz = b \Rightarrow x = y = \sqrt{b - dc}\end{aligned}$$

When $b \leq dc$ the fixed points for $x, y = 0$ and $z = \frac{d}{b}$ When $b > dc$ the fixed points are $(\pm\sqrt{b - cd}, \pm\sqrt{b - cd}, c)$

- **Sensitivity to initial conditons** Starting the system with slightly different initial conditions $(0, 0{,}1, 0)$ and $(0, 0{,}09, 0)$ we can see that after some time the two trajectories quickly diverge from each other

[8] Shows that the system presents chaos of horseshoe type.

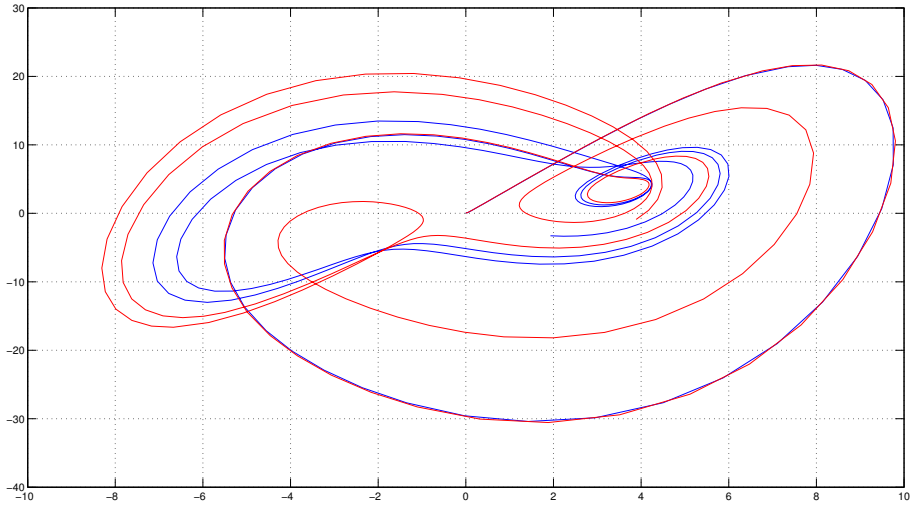

Figura 1.7: *Sensitivity to initial conditions in a Third Order Autonomous System*

II. Simulations

Simulations with Chua's System and the system proposed by [8] were used to see if any of the system follows Benford's Law. On one hand we used Simulink and MATLAB in order to produce bifurcation diagrams and set up the dimensionless differential equations. On the other hand, we used a SPICE-based circuit simulator in order to get the systems in terms of electrical components.

Chua's Circuit

- **Physical Realization** The system describing chua's System

$$\begin{aligned} \frac{G}{C1}V_2 - \frac{G'_b}{C_1}V_1 - (\frac{G_b - G_a}{C_1})E \quad & if \quad V_1 < -E \\ \frac{G}{C1}V_2 - \frac{G'_a}{C_1}V_1 \quad & if \quad -E \geq v1 \leq E \\ \frac{G}{C1}V_2 - \frac{G'_b}{C_1}V_1 - (\frac{G_a - G_b}{C_1})E \quad & if \quad V_1 > E \end{aligned}$$

  is given by the following schematic

  With the Capacitors C1=10nF C2=100nF and a 8mH Inductor given by the gyrator circuit.

- **Numerical Simulations** Using a spice based simulation software and MATLAB, several resistor values where tested, we constructed the bifurcation diagram and plotted for some R values

- **Benford Analysis** The first digit distribution was determined from the voltage measured at the terminals of C1, using a resistance value of 1860Ω, at that value, Chua's Circuit presented Chaotic Behaviour. The first digits (without leading zeroes) of the voltage values at discrete points were analyzed. We compared the first digit distribution of the dataset with the

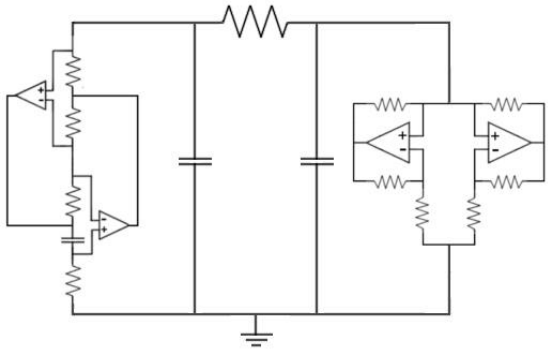

Figura 1.8: *OP-Amp Based realization of Chua's Circuit*

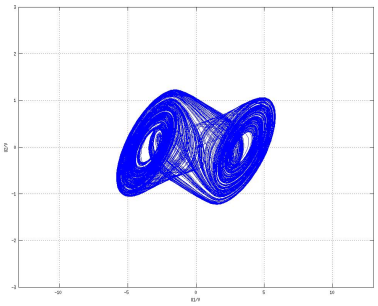

(a) *V1-V2 plane for R=1785*

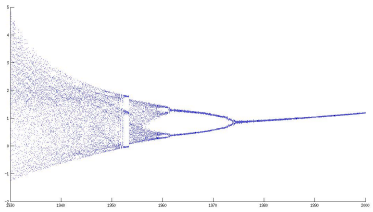

(b) *Bifurcation Diagram for Chua's Circuit*

distribution given by Benford's Law using the Mean Absolute Deviation (MAD) proposed by [2]. We got a MAD value of 0.22, with a maximum of 0.15 in order to be conformant with Benford's Law.

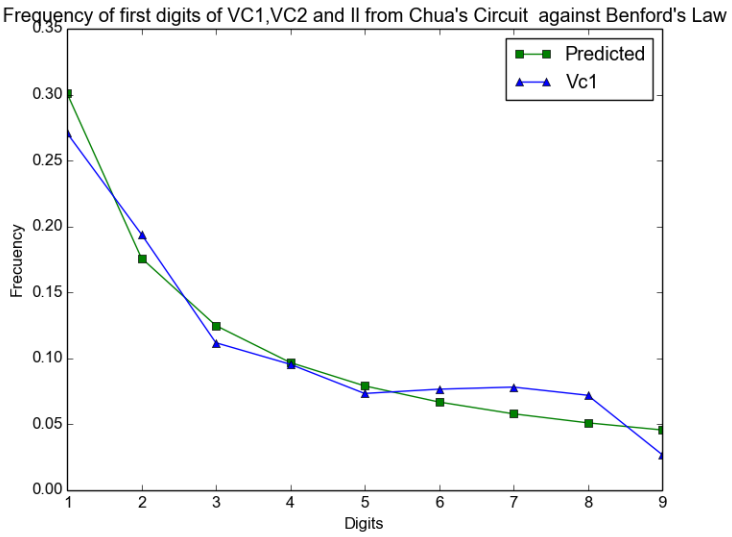

Figura 1.10: *OP-Amp Based realization of Chua's Circuit*

Three-Dimensional Autonomous Circuit

- **Physical Realization** The electronic circuit built to realise the system is shown in figure 2.4: Voltages V_x,V_y and V_z are the output voltages of the operational amplifiers representing x,y and z, $k_m = 10V$ is the fixed constant of the AD633 multipliers, so the outputs of the multipiers are $V_{xz} = V_x V_z / k_m$ and $V_{x^2} = V_x V_x / k_m$.

  Substitution of resistor values into Eqs. (1.5),(1.6),(1.7) yields:

$$\frac{dV_x}{dt} = \frac{1}{R_1 C_1}\left(V_y - V_x \frac{R_1}{R_4}\right) \tag{1.11}$$

$$\frac{dV_y}{dt} = \frac{1}{R_2 C_2}\left(\frac{V_x V_z}{k_m} - \frac{R_2}{R_6} V_y\right) \tag{1.12}$$

$$\frac{dV_z}{dt} = \frac{1}{R_3 C_3}\left(V_b\left(1 + \frac{R_3}{R_5}\right) - \frac{V_x^2}{k_m} - \frac{R_3}{R_5} V_z\right) \tag{1.13}$$

  The values for resistors and capacitor used where: $R_1 = 0{,}5\ \text{K}\Omega$, $R_2 = 10\ \text{K}\Omega$, $R_3 = 10\ \text{K}\Omega$, $R_4 = 5\ \text{K}\Omega$, $R_5 = 1{,}15\ \mathbf{M}\Omega$, $R_3 = 1\ \text{M}\Omega$, $C_1 = 100\ \text{nF}$, $C_2 = 100\ \text{nF}$, $C_3 = 10\ \text{nF}$, $V_b = 10\ \text{K}\Omega$

- **Numerical Simulations** We used SIMULINK in order to model the system and MATLAB to create the bifurcation diagram. The response of the syste with the parameters indicated above is given by figure 2.5:

  Bifurcation diagram for the z value

- **Correspondence with Benford's Law** The same methodology used in Chua's Circuit was used with this circuit, taking measurements from V_y and using the MAD test to verify conformity with the First Digit Distribution

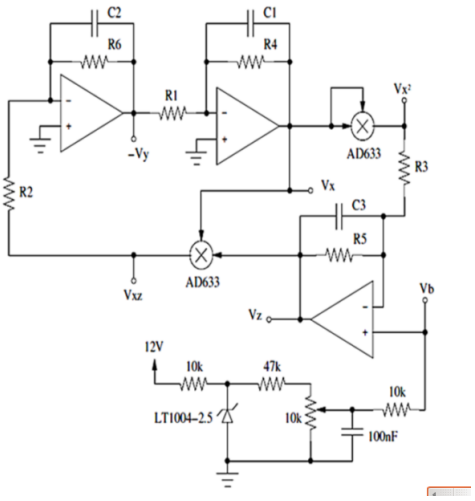

Figura 1.11: *Circuit Schematic*

For different values of d, we did a table with the respective first digit frequencies (10000 samples) and MAD test.

Leading digit	Benford Distribution	d=1/23	d=0.03	d=0.01	d=0.001	d=0.00001
1	0,3010	0,3296	0,3132	0,3166	0,2792	0,3108
2	0,1760	0,1787	0,1800	0,1801	0,1707	0,1781
3	0,1249	0,1111	0,1142	0,1196	0,1209	0,1230
4	0,0969	0,0856	0,0910	0,0894	0,0904	0,0941
5	0,0791	0,0727	0,0791	0,0765	0,0754	0,0731
6	0,0669	0,0604	0,0647	0,0672	0,0670	0,0691
7	0,0579	0,0581	0,0602	0,0567	0,0596	0,0565
8	0,0511	0,0565	0,0511	0,0493	0,0515	0,0496
9	0,0457	0,0473	0,0465	0,0446	0,0415	0,0457
MAD		0,0085	0,0042	0,0044	0,0053	0,0031

We noticed strong agreement given by Nigrini[2], next, we built the circuits and do tests measuring voltages.

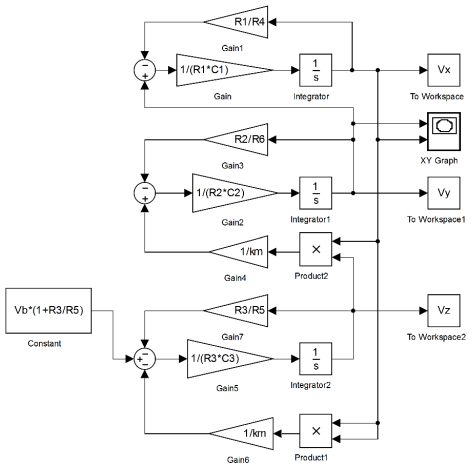

Figura 1.12: *Simulink simulation*

III. Experimental Results

Chua's Circuit

- **Methodology** We constructed the circuit using 4 TL082 I.C.'s and commercial resistors with the values used during simulation, Trimmer resistors to be able to move the resistor values of R.

  We used two oscilloscope probes to measure the voltage from the two capacitors, and did our measurements with a Tektronix DS201 Oscilloscope with a direct method sampling.

  The first digit distribution was determined from the voltage measured at the terminals of C1,varying R from 1700Ω to 1900Ωin 25Ω intervals, values in which Chua's Circuit presented chaotic behaviour. The first digits (without leading zeroes) of the voltage values at discrete points were analyzed, the oscilloscoped allowed us to take 2000 samples from a 250 μs period. We compared the first digit distribution of the dataset with the distribution given by Benford's Law using the Mean Absolute Deviation (MAD) proposed by [2].

- **Results** We put a table with the MAD results at each value of R:

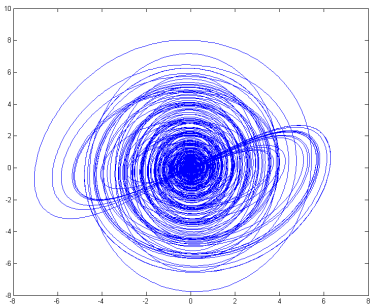

(a) *V1-V2 V_x vs V_y plot*

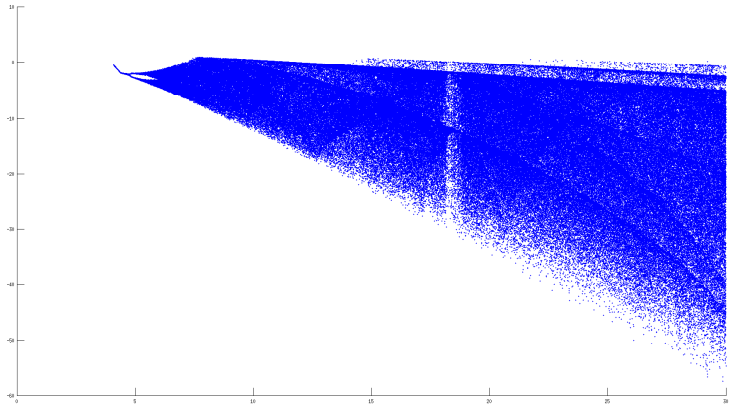

(b) *Bifurcation Diagram varying b*

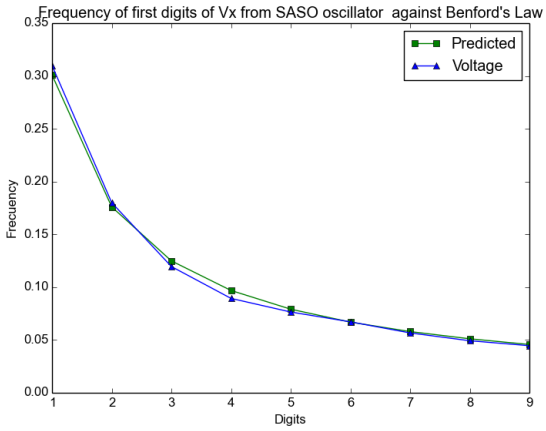

Figura 1.14: *V_x against Benford's Law*

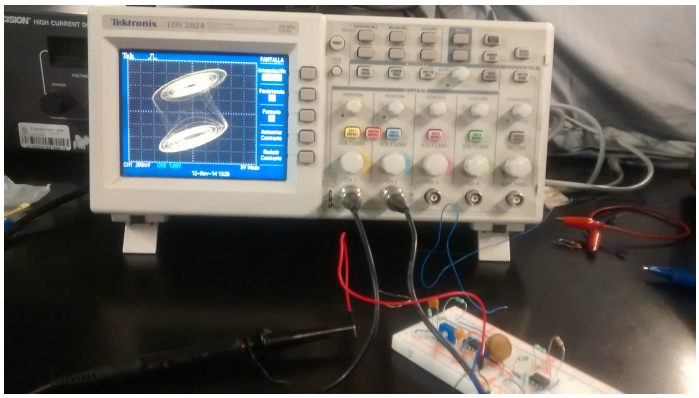

Figura 1.15: *Chua's System Breadboard*

R	VC1	VC2
1700	0.0265740826252	0.0941252615083
1725	0.0308583854254	0.0894910362566
1750	0.0225012003889	0.0937811348396
1775	0.0213932963068	0.0894482136018
1800	0.0515553953624	0.0817178075546
1825	0.0620516456615	0.0757908400412
1850	0.0801858066881	0.0616474503737
1875	0.0864648516751	0.0566898036332
1900	0.0848654579991	0.0477795566486

The closest value we got was with R=1775 measuring VC1

- **Remarks**

  We noticed that between for R between 1730 and 1775, there is a more clear First Digit Distribution according to Benford's Law, however, the measurements did not comply with MAD's Criteria which expects at most 0.015 in order to be compliant with Benford's Law.

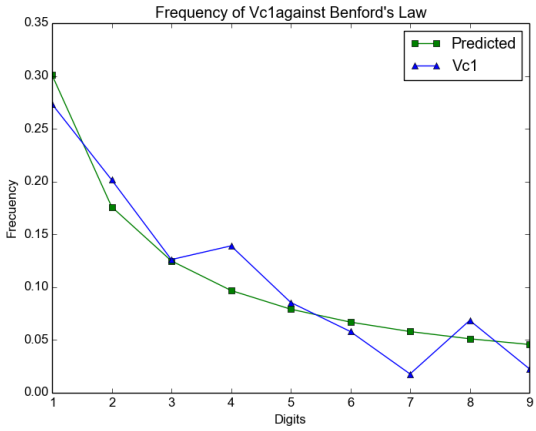

Figura 1.16: *Benford's Law against VC1*

We also took a measurement with R=2000Ω, value at which the system behaves as a quasi-periodic oscillator. we noticed that the first digit distribution is more uniform.

Takougang Circuit

- **Methodology**The circuit was connected using a standard breadboard, according to the diagram, all passive components had a nominal value equal to the ones proposed in the schematic, with a tolerance of 5 %. A regulated voltage source, set to $\pm$ 12 V was utilized to feed the active components which were the same as stated in the schematic. A third output of the regulated voltage source served to provide a stable input for the circuit (V_b). Next, a digital oscilloscope was used in order to obtain the data provided by the circuit.

  A 1 GHz band-width oscilloscope (Agilent DSO6104A) was used next, and it was configured in order to reduce random noise. The sampler uses an averaging algorithm which delivers data with less noise, and reduces the vertical resolution (as low as 0.7 mV), with the data obtained from that oscilloscope the analysis was more reliable and results confirmed what was expected from the simulations, although only 1000 samples in an interval of 10 ms were fetched.

- **Results** The first digit distribution of the voltages was taken and following the same methodology as with Chua's System, we swept through V_b and took the MAD value from each distribution

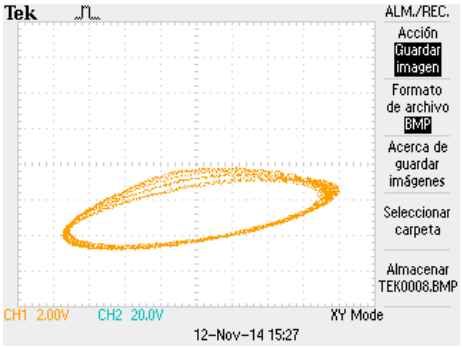

(a) *V1-V2 V_x vs V_y plot*

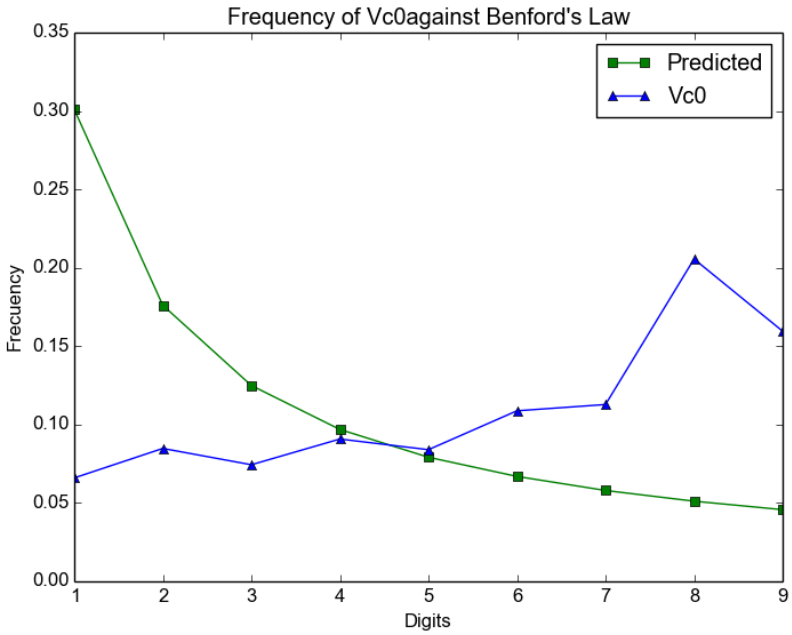

(b) *Bifurcation Diagram varying b*

V_b	V_x	V_y
82mV	0.0775279989288	0.0607280417648
92mV	0.0789296997697	0.0620760330126
102mv	0.0779822062934	0.0620098514762
112mv	0.0722551588234	0.0586329019652
117mv	0.0731369417692	0.0565637073089
122mv	0.0761361923841	0.0607646781498
127mv	0.0702382876578	0.0581541345311
132mv	0.0726371865346	0.0568562424256
137mv	0.0723923763659	0.0588608733569
142mv	0.0689722218274	0.0566979795649
147mv	0.0649140903028	0.0492049220995
152mv	0.0689575397758	0.0540809650999
157mv	0.071269709088	0.0556102788266
167mv	0.0713877270204	0.0546276659144
187mv	0.0642837364043	0.0499581746439
197mv	0.0619961498144	0.0491763886427
217mv	0.0644054740322	0.0521147934116
237mv	0.0574813303354	0.0515391121266
257mv	0.0552768884655	0.0514296383228
277mv	0.0464325092508	0.0450451557158
112mv (H-Res)	0.0126362748635	0.0149581584175
132mv (H-Res)	0.0114562387312	0.0056682935093
152mv (H-Res)	0.0106402668795	0.0143777130129
172mv (H-Res)	0.0077090293797	0.0118696485616
192mv (H-Res)	0.00801241025011	0.0120739312228

We notice we have the best agreement with Benford's Law with $V_b = 132mV$ Which gives a MAD value of 0.0056

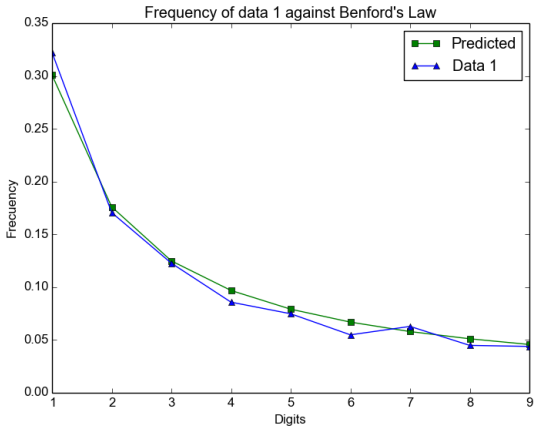

Figura 1.18: *Benford's Law against digit distribution of V_y*

- **Remarks**

Simulations from Simulink gave a better accordance with $V_b = 132mV$, however measuring without High-resolution sampling we did not obtain proper distributions, until we activated that sampling method, we got a distribution according to Benford's Law

IV. Conclusion

In the work done by Tolle [10] some dynamical systems were proposed and theye checked if the first digit distribution followed Benford's Law. We took 2 autonomous circuits which displayed chaotic behaivour and verified if they were conformant according with the criterion given by Nigrini et. al. [2]. According to our experimental results, the system which best followed the distribution whas the Third Order Autonomous System proposed by Takougang et.al [8].

Verifyng the results from [8], we notice that this circuit has a Shilnikov heteroclinic orbit, which implies by the Shilnikov Criterion that the system has horseshoe chaos. This type of chaos produces time signals called chaotic bursting oscillations (see Fig. 4.1)

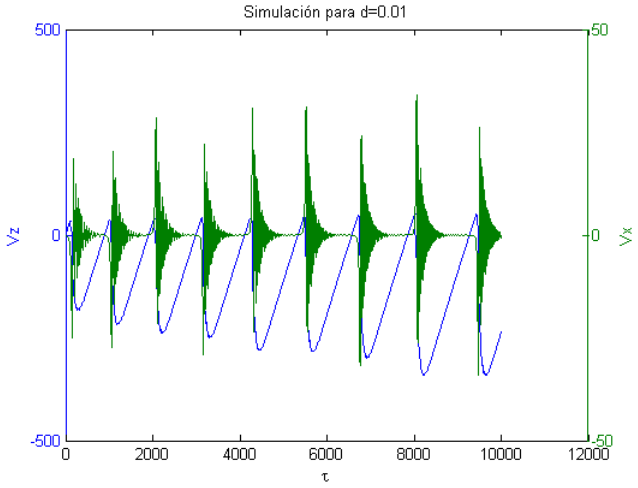

Figura 1.19: *V_y response as a function of time*

This type of oscillations are found in biological phenomena, such as Ca^2+ oscillations in non-excitable cells [11], pancreatic β cells [12] and in neurons[13] and heart oscillatons, also, the work by Kreuzer et. al. [3] indicates that brain electrical activity follows Benford's Law, so it would be interesting to see if Benford's Law could be an indicative if Real life phenomena is modelled correctly by the system if both follow Benford's Law (as it was first indicated by [10]) and also to try to verify if other systems that present this kind of oscillations also follow Benford's Law.

Bibliografía

[1] Benford Frank, *The law of anomalous numbers*. Proc. Amer. Philos. Soc. 78, (1938), 551-572.

[2] Nigrini Mark J., Mittermaier Linda J. *The use of Benford's Law as an Aid in Analytical Procedures* Auditing: A Journal of Practice & Theory, (1997), 52-67

[3] Matthias Kreuzer, Denis Jordan, PhD, Bernd Antkowiak, Berthold Drexler, Eberhard F. Kochs, and Gerhard Schneider *Brain Electrical Activity Obeys Benford's Law* Neuroscience in Anesthesiology and Perioperative Medicine, (2014), 183-191

[4] Steven H. Strogatz *Nonlinear Dynamics and Chaos, With Applications to Physics, Biology, Chemistry and Engineering, Second Edition* Westview Press, (2014), 309-191

[5] U. Parlitz *Lyapunov's Exponent from Chua's Circuit* Journal of Circuits, Systems, and Computers,Vol. 3, No.2 (1992), 507-523

[6] Michale Peter Kennedy *Experimental Chaos from Autonomous Electronic Circuits* Phil. Trans. R. Soc. Lond. A, (1995), 507-523

[7] Ayrom F., *Chaos in Chua's Circuit*, IEE Proceedings, Vol. 133, No. 6 307-312 , 1986, 307-312

[8] Sifeu Takougang Kingni, Lars Keuninckx, Paul Woafo, Guy Van der Sande, Jan Danckaert *Dissipative chaos, Shilnikov chaos and bursting oscillations in a three-dimensional autonomous system: theory and electronic implementation* Nonlinear Dynamics, 2013

[9] Torres J. et al., *How do numbers begin? (The first digit law)*, Eur. J. Phys., Vol. 28, 2007, 17-25

[10] Charles R. Tolle, Joanne L. Budzien, and Randall A. LaViolette *Do dynamical systems follow Benford's law?* Chaos: An Interdisciplinary Journal of Nonlinear Science 10, 331, 2000

[11] Perc, M., Marhl, M. *Different types of bursting calcium oscillations in non-excitable cells*, Chaos Solitons Fractals 18, 759–773 2003

[12] Sherman, A., Rinzel, J., Keizer, J. *Emergence of organized bursting in clusters of pancreatic β-cells by channel sharing*, Biophys. J. 54, 411–425, 1988

[13] *Mathematical Foundations of Neuroscience* Interdiscplinary Applied Mathematics 35, 103-126, 2009

Capítulo 2

Dinámica Agro-Socio-Ambiental en la conservación de la biodiversidad en México mediante la regulación de la calidad de la Matriz Agrícola

Alan Osorio Orduña, Sergio Naude Citalán

Resumen

Hoy en día las reservas naturales están siendo afectadas por la actividad humana. La producción agrícola no planificada adecuadamente, genera destrucción del hábitat alterando los ecosistemas, de tal forma que en ocasiones resulta en un daño irreversible.

Disminuir el impacto ambiental provocado por las zonas de cultivo cercanas a reservas naturales sin interrumpir la producción agrícola, es una de las prioridades en diferentes partes del mundo.

En base a estudios que sean realizados en los últimos años se piensa que la matriz agrícola es de vital importancia. Es útil ver de manera gráfica y numérica los efectos que el hombre causa en la naturaleza. Razón por la cual se recopilo información de diferentes fuentes, todas relacionadas con el cultivo de café en Chiapas. Los datos recopilados fueron almacenados en una base de datos, para después ser utilizados para el modelo matemático realizado con cadenas markovianas. A partir de los resultados obtenidos en el modelo se describe la proyección a futuro de la calidad de la matriz. Los parámetros considerados para determinar la calidad de la matriz fueron de distintos ámbitos, desde flora y fauna del lugar, hasta métodos de cultivo y compuestos de plaguicidas y fertilizantes.

Con este proyecto se pretende configurar los parámetros necesarios para cambiar el estado de la calidad de una matriz a otro, o por el contrario mantenerlo en un tiempo determinado.

Se realizaron programas de software para visualizar y conocer el la calidad de la matriz agrícola de las zonas de cultivos con respecto a las especies que habitan en los alrededores en un

tiempo especificado.

Para la creación y depuración del programa se usó un compilador orientado a agentes, el cual permitió ver la interacción de las especies animales con el medio.

I. Introducción

El crecimiento urbano propicia cambios en los espacios circundantes, tales como la pérdida de áreas agrícolas y forestales a favor de los ambientes urbanizados, y cambios en las estructuras socioeconómicas relacionadas con el manejo y propiedad de la tierra.

Chiapas es un estado con un fuerte crecimiento pero que aún mantiene áreas forestales, que cuentan con esquemas de protección de sus bosques.

El efecto del crecimiento urbano es complejo y no unidireccional, pues representa una fuerte presión para el cambio de uso del suelo, pero también ha permitido la reactivación de actividades agrícolas de bajo impacto y la revalorización de las áreas forestales.

Chiapas es conocido por su alta diversidad de especies de mamíferos, sin embargo, en la entidad grandes extensiones de hábitats naturales han sido modificados a zonas agrícolas, lo cual se cree que disminuye la riqueza de especies.

Por ello, el presente trabajo tiene como objetivo determinar la riqueza de suelo en zonas agrícolas del estado de Chiapas, particularmente en las que se cultiva café. Se recopiló información de las especies de flora y fauna de la región en bases de datos del gobierno estatal y federal, así como en colecciones de literatura científicas nacionales e internacionales.

II. Objetivos

- Descripción de la dinámica espacio-temporal de los factores agro-socio-ambientales relacionados con los sistemas agrícolas que impactan la calidad de la matriz agroecológica. Mediante el empleo de dinámicas Markovianas para la descripción de la evolución de la matriz agro-ecológica y considerando la interacción de territorios aledaños mediante dinámicas de agentes.

- Desarrollo de un simulador computacional capaz de analizar mediante sistemas de información geográfica y bases de datos disponibles el escenario del impacto de distintos tipos de manejo agrícola en diversos contextos socio- ambientales en la dinámica espacio-temporal de la matriz.

III. Marco Teórico

I. Cadenas de Markov

Se conoce como cadena de Márkov a un tipo especial de proceso estocástico discreto en el que la probabilidad de que ocurra un evento depende solamente del evento inmediatamente anterior. Si se conoce la historia del sistema hasta su instante actual, su estado presente resume toda la

información relevante para describir en probabilidad su estado futuro.

Si el estado X_n y los estados previos $X_1, \ldots, X_{n-1}$ son conocidos. La probabilidad del estado futuro X_{n+1}. No depende de los estados anteriores $X_1, \ldots, X_{n-1}$. Solamente depende del estado X_n.

Es decir,

- Para $n = 1, 2, \ldots$ y
- Para cualquier sucesión de estados $s_1, \ldots, s_{n+1}$.

$$P(X_{n+1} = s_{n+1} | X_1 = s_1, X_2 = s_2, \ldots, X_n = s_n) = P(X_{n+1} = s_{n+1} | X_n = s_n) \quad (2.1)$$

II. Matriz de transición

En matemáticas, una matriz de Markov es una matriz utilizada para describir las transiciones en una cadena de Markov. Existen varias definiciones y tipos de matriz estocástica:

- Una matriz estocástica derecha es una matriz cuadrada cada una de cuyas filas está formada por números reales no negativos, sumando cada fila 1.
- Una matriz estocástica izquierda es una matriz cuadrada cada una de cuyas columnas está formada por números reales no negativos, sumando cada columna 1.
- Una matriz doble estocástica es una matriz cuadrada donde todos los valores son no negativos y todas las filas y columnas suman 1.

Un proceso de Markov en que el sistema posee n estados posibles, dados por los números $1, 2, 3, \ldots, n$. Denotemos p_{ij} a la probabilidad de que el sistema pase al estado j después de cualquier ensayo en donde su estado era i antes del ensayo. Los números p_{ij} se denominan probabilidades de transición y la matriz $n \times n$ $P = (p_{ij})$ se conoce como matriz de transición del sistema.

La suma $1 \ldots p_{i1} + p_{i2} + p_{in} = 1$. Esta suma representa la probabilidad de que el sistema pase a uno de los estados $1, 2, \ldots, n$ dado que empieza en el estado i. Ya que el sistema ha de estar en uno de estos n estados, la suma de probabilidades debe ser igual a 1. Esto significa que los elementos en cualquier renglón de la matriz de transición deben sumar 1. Cada elemento $p_{ij} \geq 0$.

De la misma manera, puede definirse un vector estocástico como un vector cuyos elementos están formados por números reales no negativos que suman 1. Así, cada fila (o columna) de una matriz estocástica es un vector de probabilidad, también llamados vectores estocásticos.

IV. Simulación

Dentro de la simulación son usados dos programas principalmente. El primero de ellos es Matlab con una interfaz gráfica, el segundo es el programa de desarrollo de ambientes Netlogo.

La interfaz gráfica implementada en Matlab permite ingresar los datos de la matriz de transición. Cada elemento de la matriz y el vector de condiciones iniciales son introducidos manualmente por el usuario. Después mediante un algoritmo de iteraciones entre el vector de condiciones iniciales y la propia matriz de transición, se obtiene un vector de salida. Éste último nos indica en qué tipo de clasificación se encuentra la matriz.

Primero se introducen las condiciones iniciales en forma de vector fila. Dichas condiciones indican la calidad de la matriz en un inicio, en escala de 0 a 1, siendo 1 excelente calidad. En base a diversas propiedades con las que cuenta la matriz es como se le asignan las componentes al vector. En el presente trabajo los factores considerados fueron:

- Tipo de cultivo.
- Fertilizantes y/o plaguicidas.
- Calidad de sombra.

La Figura 2.1 muestra la interfaz en Matlab

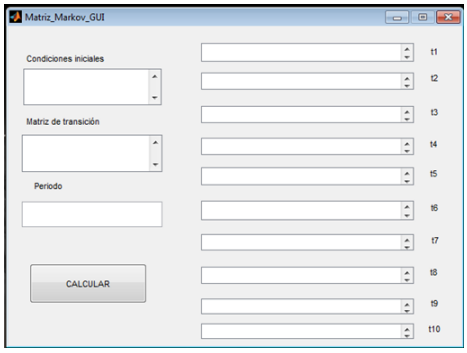

Figura 2.1: *Interfaz gráfica- Matriz de Markov*

La matriz de transición nos condensa las probabilidades de un estado a otro. A través de ésta matriz se puede observar el comportamiento representado por una cadena de Markov. Es decir, las propiedades de cambio entre los estados de la matriz agrícola.

Finalmente el periodo (en años) acota la escala de tiempo en la que se evalúa la matriz. Limitado por la información disponible, la proyección sólo se puede hacer máximo a 10 años.

El vector de condiciones iniciales es el siguiente:

$$\begin{bmatrix} 0.1 & 0.5 & 0.9 \end{bmatrix}$$

La matriz de transición fijada es la siguiente:

$$\begin{bmatrix} 0.3 & 0.6 & 0.7 \end{bmatrix}$$
$$\begin{bmatrix} 0.1 & 0.3 & 0.8 \end{bmatrix}$$
$$\begin{bmatrix} 0.4 & 0.6 & 0.6 \end{bmatrix}$$

El programa en Netlogo muestra de manera gráfica la interacción de la matriz agrícola con especies animales. Además presenta el impacto que tienen distintos métodos de cultivo en la población de la fauna silvestre. La Figura 2.2 muestra el programa de Netlogo en ejecución.

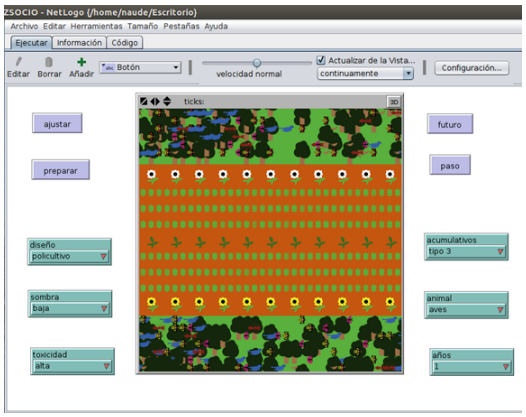

Figura 2.2: *Interfaz en Netlogo*

V. Manual de software de simulación la calidad de la matriz agrícola de café

1. Se seleccionan los parámetros de la zona agrícola.
2. Tipo de diseño, sombra, toxicidad y acumulativos.
3. Se da clic en ajustar para que muestre la zona agrícola con los parámetros deseados.
4. Se selecciona el animal con el que se pretenda visualizar como atravesara la zona agrícola con los parámetros descritos anteriormente.
5. Se presiona el botón "preparar" para ajustar el entorno y las variables que van estar interactuando durante el paso de la especie animal por la zona agrícola.
6. Se presiona el botón "paso" para que avancen cierta cantidad de espacio los animales por la zona agrícola hasta que salgan de ella.
7. Se colocan los nuevos parámetros así como la cantidad de años que a la que se quiere visualizar como se verá la matriz a tiempo futuro con los nuevos parámetros.

VI. Conclusiones

Se prueba la importancia de la calidad de la matriz agrícola en su entorno (en este caso es específicamente la relacionada con el cultivo de café).

Se visualiza de manera gráfica y numérica el impacto de la matriz con su alrededor en un tiempo finito a través de la modificación de ciertos parámetros.

Se encuentra la ponderación de los parámetros que puede modificar de manera directa el hombre sobre la matriz agrícola en las zonas de cultivo de café.

Se logra visualizar los rangos de valores que deben tener los parámetros para reducir los daños generados por el hombre mientras realiza una actividad agrónoma, en este caso el cultivo de café.

Bibliografía

[1] I. I. P. Armbrecht and J. Vandermeer, "Enigmatic biodiversity correlations: Ant diversity responds to diverse resources.," *Science 304:284-286*, 2004.

[2] N. A. Beecher, R. J. Johnson, J. R. Brandle, R. M. Case, and L. J. Young, "Agroecology of birds in organic and non organic farmland," *Conservation Biology 16:1620-1631*, 2002.

[3] A. Berggren, B. Birath, and O. Kindvall, "Effect of corridors and habitat edges on dispersal behavior, movement rates, and movement angles in roesel's bush-cricket (metrioptera roeseli)," *Conservation Biology 16:1562-1569*, 2002.

Capítulo 3

Interacción entre el Bienestar Psicológico y el Paisaje Acústico